J. Fluid Mech. (1999), *vol.* 381, *pp.* 121–139. Printed in the United Kingdom

© 1999 Cambridge University Press

Linear growth in two-fluid plane Poiseuille flow

By M. J. SOUTH AND A. P. HOOPER

Faculty of Computer Studies and Mathematics, University of the West of England, Bristol BS16 1QY, UK
email: alison.Hooper@uwe.ac.uk

(Received 29 May 1997 and in revised form 10 September 1998)

In recent years a new paradigm has emerged in linear stability theory due to the recognition of the importance of non-normality in the Orr–Sommerfeld equation as derived from the method of normal modes. For single-fluid flows it has been shown that it is possible for the kinetic energy of certain stable mode combinations to grow transiently before decaying to zero. We look again at the linear stability of two-fluid plane Poiseuille flow in two dimensions, concentrating on transient growth and its dependence on the viscosity and depth ratio. The procedure is to solve the stability equations numerically and consider disturbances defined as a sum of the least stable eigenmodes (not just the least stable interfacial mode). It is found that the variational method used to find maximum growth cannot be based upon the kinetic energy of the flow only and that interface deflection must be included in the formulation. We show which modes are necessary for inclusion in the disturbance expression and find that the interfacial mode does not make a significant contribution to possible energy growth. We examine the magnitude of maximum growth and the nature of the disturbances that lead to this growth. The linear energy rate equation shows that at moderate Reynolds numbers the mechanism responsible for the largest two-fluid growth is transfer of energy from the basic flow via the Reynolds stresses. The energy transfer is facilitated by streamline tilting that can be seen at the channel walls or at the interface. A similar effect has been found in single-fluid plane Poiseuille flow.

1. Introduction

Hydrodynamic stability studies of shear flows of two superposed fluids have concentrated on the behaviour of the interfacial mode. This mode is due to the presence of the interface and in flow configurations in which gravity is absent or acts parallel to the interface, its behaviour is governed both by the viscosity and/or density jump across the interface and the proximity of the boundary walls. The stability equations for two-fluid flows admit an infinite number of discrete eigenvalues and eigenmodes and the interfacial mode is usually the leading eigenmode. Linear stability studies have concentrated on the determination of the eigenvalue of the interfacial mode and non-linear studies have looked at the reaction of the interfacial mode to finite-amplitude effects.

Recent linear stability studies of single-fluid shear flows have questioned the validity of considering the leading eigenmode and its growth rate in isolation from the remainder of the spectrum of eigenmodes, see Trefethen *et al.* (1993), Reddy & Henningson (1993), Farrell (1988), Butler & Farrell (1992). They show that even though the leading eigenmode is stable, linear growth can still occur which results in energy growth of $O(10)$ for two-dimensional disturbances. The growth is due to the

https://doi.org/10.1017/S0022112098003577 Published online by Cambridge University Press

non-normality of the Orr–Sommerfeld operator. The initial disturbance which can achieve this kind of growth is a series expansion of all the eigenmodes and typically is the conjugate adjoint of the leading eigenmode.

In this paper we re-examine the linear stability of two-fluid shear flows from the perspective of disturbance energy growth. We want to determine the magnitude of the maximum energy growth possible and show which eigenmodes make up the initial disturbance which leads to this growth. We anticipate that the interfacial mode will play a significant role in the determination of energy growth.

In §2 we set up the governing equations for channel flow of two superposed viscous fluids. We then extend the single-fluid energy equations to include two fluids but we find that a simple extension of the energy equations leads to problems of non-convergence. The problems of non-convergence are caused by the interfacial mode. The behaviour of this mode is totally different from the other eigenmodes. In particular, in the single-fluid limit of the two-fluid flow configuration (when the parameters of both fluids are the same), the governing stability equations admit a solution for the interfacial mode with zero velocity field but an unspecified amplitude of the disturbed interface. Thus unlike the eigenmodes in single-fluid flows which are completely defined by the eigenfunction $\phi(y)$, the eigenmodes in two-fluid flows are defined by the three-component vector $(\phi(y), \chi(y), h)^T$ where ϕ and χ are the eigenfunctions of the Orr–Sommerfeld equations in the upper and lower fluids respectively and h is the amplitude height of the disturbed interface. In the single-fluid limit of the two-fluid configuration, this normalized interfacial eigenmode is equal to $(0, 0, 1)^T$. An Hermitian inner product and corresponding 'energy' norm must take into account the amplitude of the disturbed interface (Y. Renardy, private communication). We overcome the problem of non-convergence by using an inner product defined by Renardy (1987*a*) which explicitly includes the effect of the interfacial amplitude in the positive definite form of $|h|^2$. This leads to a modified 'energy' norm for the two-fluid system which we call the h-norm. We note that Davis & Homsy (1980) introduce a similar generalized energy functional in their work on energy stability of free surface flows, see their equation (7.6).

We know from Hooper & Grimshaw (1996) that in single-fluid flows, the initial disturbance that leads to maximum growth is closely associated with the adjoint of the leading eigenmode. In §3, we study eigenmodes of the adjoint Orr–Sommerfeld equation for two fluids. We find the biorthogonality condition which links the eigenmodes of the Orr–Sommerfeld equation and the adjoint eigenmodes and note similarities between this equation, the energy rate equation and the inner product required for the h-norm. We are thus able to show that the explicit $|h|^2$ term included in the definition of the h-norm emulates the disturbance energy growth due to the presence of the interface in two-fluid flows. We conclude from this that the main mechanism for growth defined by the h-norm must be the Reynolds stress term of the energy rate equation.

We present results for the energy growth of two-fluid configurations in §4. We maximize growth using the h-norm and then isolate the growth of the disturbance kinetic energy from the final result. Good qualitative agreement is found between single-fluid systems and the corresponding two-fluid configuration when taken to the single-fluid limit. The agreement is further enhanced by using a simple modification of the h-norm which still produces convergent results but which places more emphasis on the kinetic energy component and less emphasis on the $|h|^2$ component of the h-norm.

We find that the disturbance which leads to maximum energy growth has closed

https://doi.org/10.1017/S0022112098003577 Published online by Cambridge University Press

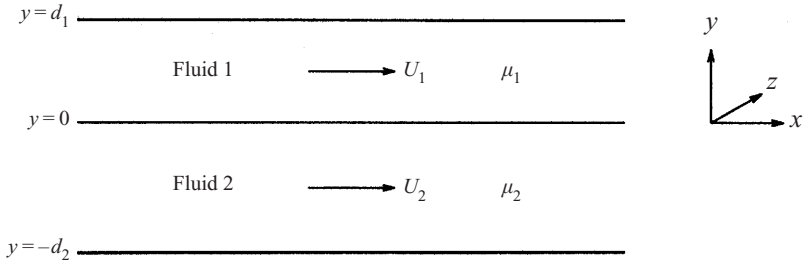


FIGURE 1. The two-fluid flow configuration.

streamlines which are tilted against the mean flow. It seems that this streamline tilting mechanism enhances transfer of energy via the Reynolds stress to the two-dimensional disturbance in two-fluid flows. The same mechanism has been found in single-fluid shear flows.

2. Formulation of the governing equations

The flow consists of two immiscible, incompressible Newtonian fluids of equal density, one on top of the other between two horizontal plates (see figure 1). The fluids are of different viscosities (μ_i) and have different depths (d_i) where $i = 1, 2$. We take surface tension to be zero.

The basic flow is parallel shear flow, $\boldsymbol{u} = (U_i(y), 0, 0)$, $i = 1, 2$, driven by a constant pressure difference in the x-direction, see figure 1. The governing equations are non-dimensionalized with respect to the depth and viscosity of fluid 1 and the maximum speed of the basic flow ($U_{\max}$) to give the following parameters of the flow: the viscosity ratio, $m = \mu_2/\mu_1$; depth ratio, $n = d_2/d_1$; and Reynolds number, defined as $R = U_{\max} d_1/\nu_1$. (In previous studies the speed of the interface, U_0, has been taken to be the representative speed of the flow and velocity is non-dimensionalized with respect to U_0 but some flow parameters m and n yield a basic flow where $U_{\max} \gg U_0$. This means that the speed of the interface, U_0, is not representative of the speed of the basic flow.) Hence the non-dimensional basic flow is given by

$$U_1(y) = \frac{1}{\tilde{U}_{\max}} \left\{ 1 + \frac{(m - n^2)}{(n^2 + n)} y - \frac{(m + n)}{(n^2 + n)} y^2 \right\}, \quad 0 \leqslant y \leqslant 1, \tag{2.1a}$$

$$U_2(y) = \frac{1}{\tilde{U}_{\max}} \left\{ 1 + \frac{(m - n^2)}{m(n^2 + n)} y - \frac{(m + n)}{m(n^2 + n)} y^2 \right\}, \quad -n \leqslant y \leqslant 0, \tag{2.1b}$$

where

$$\tilde{U}_{\max} = 1 + \frac{(m - n^2)^2}{4(n^2 + n)(m + n)} \quad \text{if} \quad m > n^2$$

and

$$\tilde{U}_{\max} = 1 + \frac{(m - n^2)^2}{4m(n^2 + n)(m + n)} \quad \text{if} \quad m < n^2.$$

We examine two-dimensional disturbances only and assume that the disturbance has an x and t dependence of the form $\exp[\mathrm{i}\alpha(x - ct)]$ where α is the dimensionless wavenumber of the disturbance in the streamwise direction. The streamfunction in

https://doi.org/10.1017/S0022112098003577 Published online by Cambridge University Press

each fluid, Φ_k, $k = 1, 2$, satisfies the Orr–Sommerfeld equations

$$\phi^{\mathrm{iv}} - 2\alpha^2\phi'' + \alpha^4\phi = \mathrm{i}\alpha R[(U_1 - c)(\phi'' - \alpha^2\phi) - U_1''\phi], \tag{2.2a}$$

$$\chi^{\mathrm{iv}} - 2\alpha^2\chi'' + \alpha^4\chi = \frac{\mathrm{i}\alpha R}{m}[(U_2 - c)(\chi'' - \alpha^2\chi) - U_2''\chi], \tag{2.2b}$$

where the prime indicates differentiation with respect to y, and

$$\{\Phi_k\} = \begin{cases} \{\phi(y)\}\mathrm{e}^{\mathrm{i}\alpha(x-ct)} & \text{in fluid 1} \\ \{\chi(y)\}\mathrm{e}^{\mathrm{i}\alpha(x-ct)} & \text{in fluid 2.} \end{cases}$$

The disturbance is subject to eight boundary conditions which are

$$\phi(1) = \phi'(1) = 0, \tag{2.3a}$$

$$\chi(-n) = \chi'(-n) = 0. \tag{2.3b}$$

There is continuity of velocity and stress at the interface. Thus we require at $y = 0$

$$\phi(0) = \chi(0), \tag{2.3c}$$

$$\phi'(0) + hU_1'(0) = \chi'(0) + hU_2'(0), \tag{2.3d}$$

$$\phi''(0) + \alpha^2\phi(0) = m\{\chi''(0) + \alpha^2\chi(0)\}, \tag{2.3e}$$

$$\phi'''(0) - 3\alpha^2\phi'(0) = m\left(\chi'''(0) - 3\alpha^2\chi'(0)\right). \tag{2.3f}$$

The term h in equation (2.3) is the amplitude of the perturbed interface which is perturbed from $y = 0$ to $y = h\mathrm{e}^{\mathrm{i}\alpha(x-ct)}$ by the disturbance. The kinematic condition at the interface gives

$$h = \frac{\phi(0)}{c - U(0)}. \tag{2.3g}$$

We define a new Reynolds number to be $R' = dU_{\max}/\bar{\nu}$, where d is the half channel width and $\bar{\nu}$ is the mean averaged kinematic viscosity, to enable comparison between results for single-fluid flows and two-fluid flows. In terms of our old Reynolds number ($R = d_1 U_{\max}/\nu_1$),

$$R' = \frac{(1+n)^2}{2(1+nm)}R. \tag{2.4}$$

With the new standard length dimension, $d = (d_1 + d_2)/2$, we define a scaled wavenumber $\alpha' = \alpha(n+1)/2$. Results for two-fluid flows are presented in terms of R' and α'.

2.1. *The energy method for two-fluid flows*

The method used to find the energy growth in two-fluid flows is an extension of the method used to find energy growth in single-fluid flows (see Hooper & Grimshaw 1996). Let the streamfunction of a general disturbance at fixed value of α be given by $v(y,t)\mathrm{e}^{\mathrm{i}\alpha x}$ where

$$v(y,t) = \sum_{n=0}^{K} a_n \Phi_n(y)\mathrm{e}^{-\mathrm{i}\alpha c_n t} \quad \text{with} \quad \Phi_n = \begin{cases} \phi_n, & y > 0 \\ \chi_n, & y < 0. \end{cases} \tag{2.5}$$

The functions (ϕ_n, χ_n) are eigenmodes of the equations (2.2*a*) and (2.2*b*) with eigenvalues $\{c_n\}$. The eigenmode (ϕ_0, χ_0) is the interfacial mode and the modes (ϕ_n, χ_n) for $n > 0$ can be clearly identified with the shear modes of single-fluid flow as $m \to 1$.

https://doi.org/10.1017/S0022112098003577 Published online by Cambridge University Press

The energy of the disturbances in two-fluid flows leads to the following norm:

$$\|v\|_o^2 = \int_0^1 \left|\frac{\mathrm{d}\phi}{\mathrm{d}y}\right|^2 + \alpha^2|\phi|^2\mathrm{d}y + \int_{-n}^0 \left|\frac{\mathrm{d}\chi}{\mathrm{d}y}\right|^2 + \alpha^2|\chi|^2\mathrm{d}y. \tag{2.6}$$

Since $v(y,t)$ is written as the finite series expansion of eigenmodes the energy norm, $\|v\|_o^2$, can be written in the matrix form, $\boldsymbol{a}^*\boldsymbol{E}^*\boldsymbol{H}\ \boldsymbol{E}\boldsymbol{a}$ where

$$\boldsymbol{a} = \begin{pmatrix} a_1 \\ \vdots \\ a_K \end{pmatrix}, \quad \boldsymbol{E} = \begin{pmatrix} \mathrm{e}^{-\mathrm{i}\alpha c_1 t} & 0 & 0 \\ 0 & \ddots & 0 \\ 0 & 0 & \mathrm{e}^{-\mathrm{i}\alpha c_K t} \end{pmatrix}$$

and the ijth component of the matrix $\boldsymbol{H}$ is

$$H_{ij} = (\Phi_i, \Phi_j)_o = \int_0^1 \frac{\mathrm{d}\overline{\phi_i}}{\mathrm{d}y}\frac{\mathrm{d}\phi_j}{\mathrm{d}y} + \alpha^2\overline{\phi_i}\phi_j\,\mathrm{d}y + \int_{-n}^0 \frac{\mathrm{d}\overline{\chi_i}}{\mathrm{d}y}\frac{\mathrm{d}\chi_j}{\mathrm{d}y} + \alpha^2\overline{\chi_i}\chi_j\,\mathrm{d}y. \tag{2.7}$$

The greatest possible growth in energy is given by the function $G(t)$ where

$$G(t) = \sup_{\|v(0)\|^2 \neq 0} \frac{\|v(t)\|^2}{\|v(0)\|^2}; \tag{2.8}$$

$\|v(t)\|^2$ is defined in (2.6). $G(t)$ is equivalent to finding the largest eigenvalue of the generalized eigenvalue problem,

$$\boldsymbol{E}^*\boldsymbol{H}\boldsymbol{E}\boldsymbol{a} = \mu\boldsymbol{H}\boldsymbol{a}.$$

For further details see Reddy & Henningson (1993) and Hooper & Grimshaw (1996).

For single-fluid Poiseuille flow, the eigenvalues are distributed along three branches (usually denoted A, P and S branches, see Mack 1976) which meet at a confluence point. Reddy & Henningson noted that in single-fluid Poiseuille flow, $G(t)$ converges when the finite sum $v(y,t)$ includes all the least stable modes up to and including the modes around the confluence point of the A, P and S branches. The eigenvalues of the single-fluid limit of two-fluid Poiseuille flow ($m \to 1$) are exactly the same as those for single-fluid Poiseuille flow except that there is an additional eigenvalue at $c = U(0)$ which is associated with the interface. Eigenvalue plots for two-fluid Poiseuille flow, when both fluids do not have the same viscosity, have a similar distribution except that the S branch splits into two almost parallel branches (which we denote S_1 and S_2), see figure 2.

The growth function, $G(t)$ for two-fluid flow when $m = 2$, $n = 1$, $R' = 1000$ and $\alpha' = 1$ is shown in figure 3. Note that $G(t)$ does not converge to a finite limit as K increases, where K is the number of modes included in the finite sum $v(y,t)$ of equation (2.5), and non-convergence is most apparent at large time. This problem of non-convergence is the result of including the interfacial mode in our expression for $v(y,t)$ in equation (2.5) and is visible for all two-fluid configurations. If we omit the interfacial mode and construct $G(t)$ from an expression made up of modes $1 \cdots K$ (as opposed to $0 \cdots K$), where K is sufficiently large to ensure convergence in single-fluid Poiseuille flow (e.g. $K = 20$ when $\alpha R = 1000$), then we recover a convergent curve $G(t)$ that is similar to the single-fluid energy growth curve. We had anticipated that the effect of the interface on the energy growth of two-fluid flows would be correctly included by defining the disturbance $v(y,t)$ to comprise the interfacial eigenmode as well as the first K leading shear modes. The non-convergence of $G(t)$ shows that the norm used in its construction is insufficient to find the energy of two-fluid flow.

https://doi.org/10.1017/S0022112098003577 Published online by Cambridge University Press

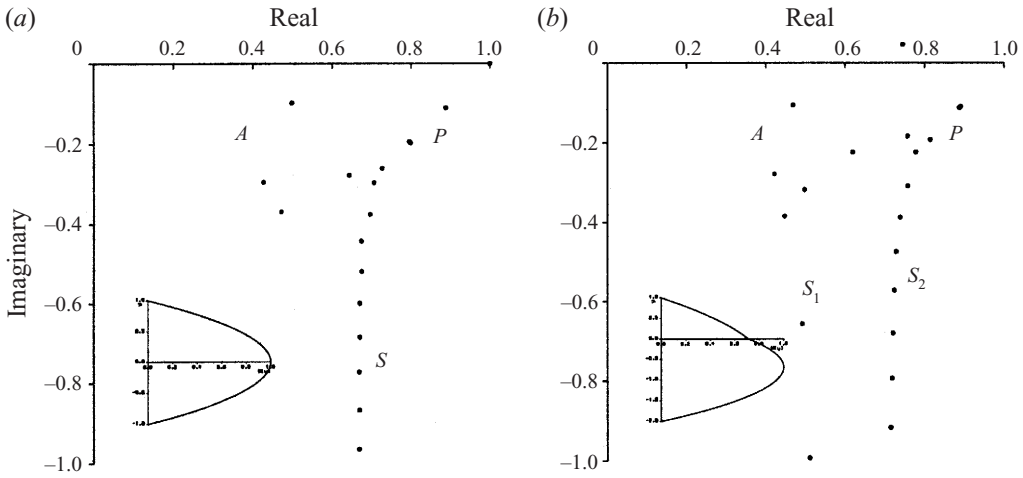


FIGURE 2. Basic flow profile and complex eigenvalues of two-fluid plane Poiseuille flow for two different flow configurations when $R' = 1000$ and $\alpha' = 1$: (*a*) $m = 1,\ n = 1$; (*b*) $m = \frac{1}{2},\ n = 2$.

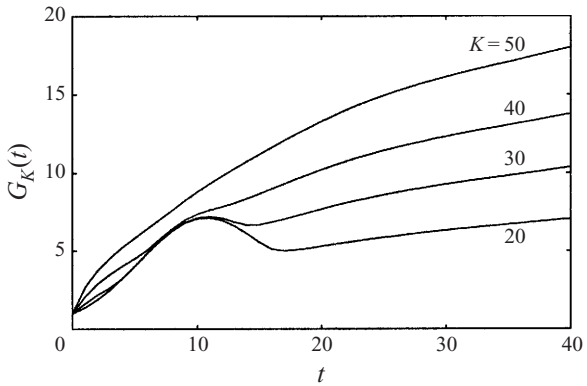


FIGURE 3. Non-convergence in the original two-fluid growth function, $G_K(t)$ when $m = 2$, $n = 1$, $R' = 1000$, $\alpha' = 1$ and K denotes the number of modes in the expansion for $v(y, t)$ in equation (2.5).

If we replace the energy norm by the L_2 norm we still have the same problem of non-convergence.

The computational explanation for non-convergence is found by inspection of the energy matrix $\boldsymbol{H}$ that is constructed when we use single-fluid energy norm. We contrast $\boldsymbol{H}$ with the matrix produced when we use the two-fluid norm $\|.\|_o$. A simplified view of the matrix $\boldsymbol{H}$ constructed using the single-fluid energy norm has the form

$$\boldsymbol{H} = \left(\begin{array}{c|c} \boldsymbol{H}_1 & \mathbf{0} \\ \hline \mathbf{0} & \boldsymbol{I} \end{array} \right). \tag{2.9}$$

$\boldsymbol{H}_1$ is a square matrix that includes all of the inner product sums for eigenvectors that are not orthogonal. Once the rank of $\boldsymbol{H}$ exceeds that of $\boldsymbol{H}_1$, the function $G(t)$ converges.

All of the two-fluid eigenvalues, other than the interfacial eigenvalue, can be associated with the single-fluid eigenvalues at equivalent Reynolds number and wavenumber. The interfacial mode which corresponds to the interfacial eigenvalue is

https://doi.org/10.1017/S0022112098003577 Published online by Cambridge University Press

a completely different type of mode from that of the shear modes. It is not orthogonal with respect to the inner product defined in equation (2.6) to any shear mode. Therefore for any given two-fluid configuration such as that which is used to generate figure 3

$$\boldsymbol{H} = \left(\begin{array}{c|cc} 1 & \boldsymbol{h}_0 & \\ \hline \boldsymbol{h}_0^T & \boldsymbol{H}_1 & \boldsymbol{0} \\ & \boldsymbol{0} & \boldsymbol{I} \end{array}\right), \tag{2.10}$$

where $\boldsymbol{h}_0$ is a $1 \times \kappa$ vector whose elements are all non-zero (the matrix $\boldsymbol{H}$ is of degree $K+1$). For the two-fluid growth function to converge, a norm must be chosen to give a partitioned form of $\boldsymbol{H}$ similar to that shown in equation (2.9).

A physical explanation of the non-convergence of $G(t)$ can be derived from examination of the energy rate equation. The energy rate equation for two-fluid flows has the form

$$\frac{\mathrm{d}}{\mathrm{d}t}E(t) = -P(t) - D(t) + I(t). \tag{2.11}$$

where $P(t)$ is the Reynolds stress term,

$$\mathrm{Re}\left\{\int_0^1 u_1^* v_1 \frac{\mathrm{d}U_1}{\mathrm{d}y}\mathrm{d}y + \int_{-n}^0 u_2^* v_2 \frac{\mathrm{d}U_2}{\mathrm{d}y}\mathrm{d}y\right\},$$

$D(t)$ represents the viscous dissipation term

$$\frac{1}{R}\int |e_{ij}|^2 \mathrm{d}y$$

and $I(t)$ represents the transfer of energy to the disturbance due to the presence of the interface and equals

$$\mathrm{Re}\left\{\frac{1}{R}\,(u_2^* - u_1^*)T_{12}|_{y=0}\right\},$$

where (u_i, v_i) is the disturbance velocity of the fluid i and T_{12} represents the disturbance tangential stress at the interface. The viscous dissipation term always reduces the energy of the disturbance but the terms $P(t)$ and $I(t)$ can be either positive or negative and both represent a mechanism by which the energy of the disturbance can grow. In previous studies of the energy of two-fluid systems, see Joseph (1988), the interfacial term has been a particularly difficult term to deal with in that unlike the Reynolds stress term, it cannot be bounded in terms of the square of the velocity. We note that it is this term, $I(t)$, which accounts for the energy of the perturbed interface and hence we want to include a positive definite term related to $I(t)$ in the energy norm construction of $G(t)$.

In a private communication Yuriko Renardy points out that the problem of non-convergence is a result of not examining the energy of the whole system and specifically not including the energy of the perturbed interface in the problem. The eigenvector in two-fluid problems consist of two important properties: its velocity field defined by $\phi(y)$ and $\chi(y)$ and its interfacial amplitude h, defined in (2.3). The inner product defined in (2.7) does not take into account the interfacial amplitude. We note that as $m \to 1$, the velocity field of the interfacial mode tends to zero but its interfacial amplitude becomes unspecified and can be any constant. Normalization of the eigenvector gives a unit interfacial height. This problem is discussed by Yih

https://doi.org/10.1017/S0022112098003577 Published online by Cambridge University Press

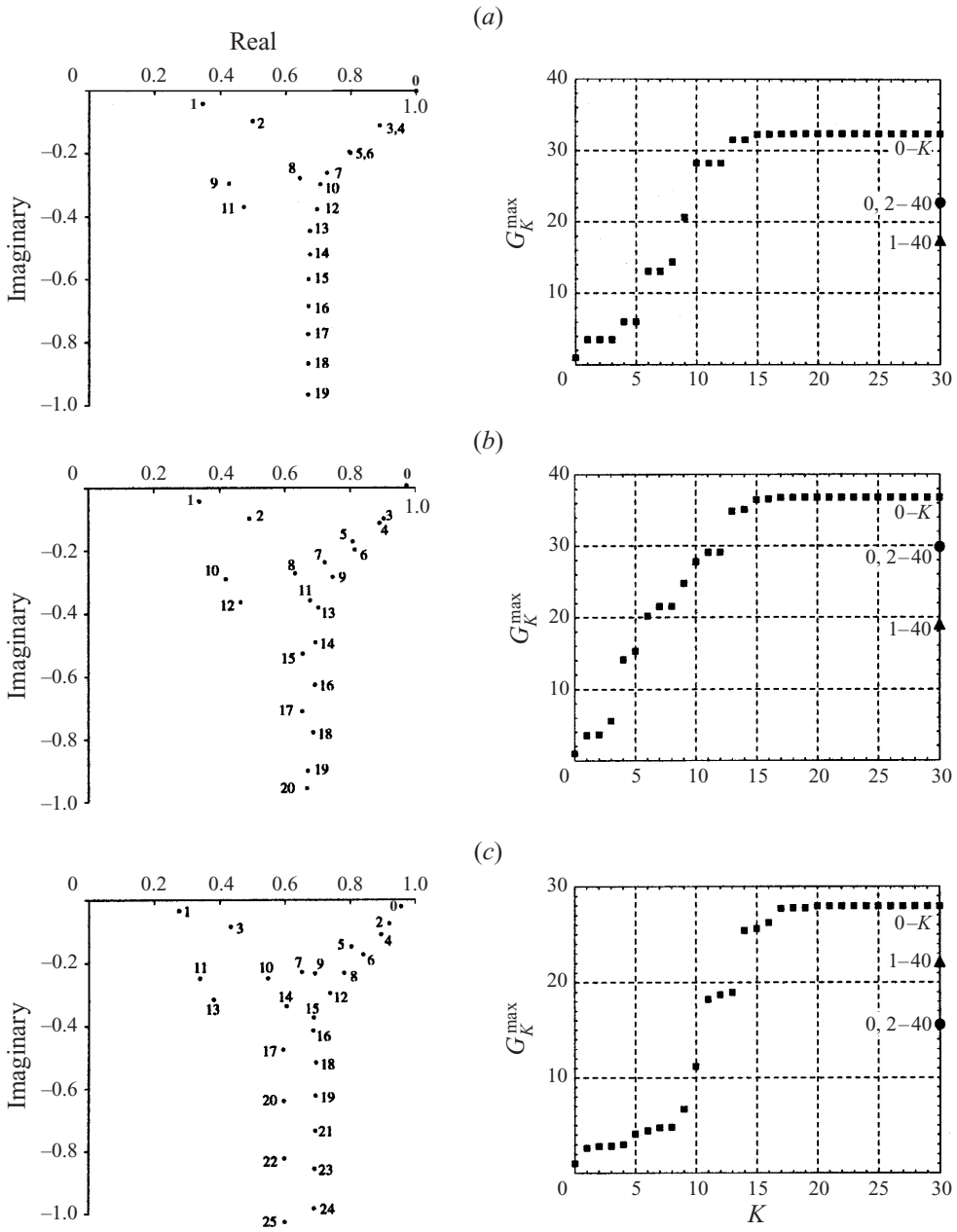


FIGURE 4. Eigenvalue plots (where the dots denote the complex values of c_j) for different values of m and n and corresponding values of $G_K^{\max}$ when $G_K^{\max}$ is calculated using 0–K modes: ■; interface mode excluded, ▲; leading shear mode excluded, •. $R' = 1000$ and $\alpha' = 1$. (*a*) $m = 1,\ n = 1$; (*b*) $m = 2,\ n = 1$; (*c*) $m = 10,\ n = 5$.

(1967). We must consider eigenvectors $\boldsymbol{\Phi}$ of two-fluid problems as consisting of three components $(\phi, \chi, h)^T$. Hence in the single-fluid limit of the two-fluid problem, the interfacial eigenvector equals $(0, 0, 1)^T$. We define an inner product which makes explicit use of the extra component in the eigenvector and use the inner product given

https://doi.org/10.1017/S0022112098003577 Published online by Cambridge University Press

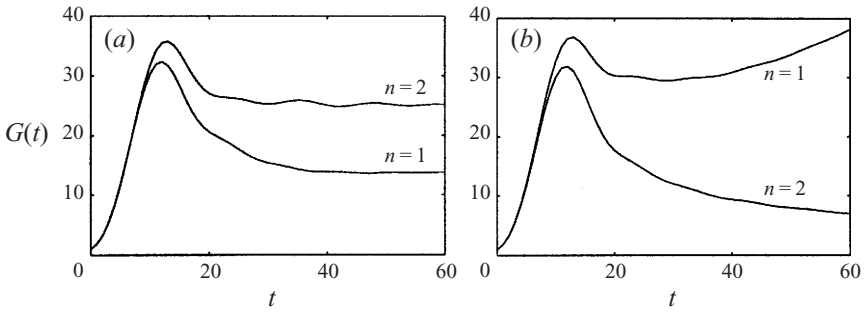


FIGURE 5. The h-norm growth function $G(t)$ for four different fluid configurations when $R' = 1000$ and $\alpha' = 1$. The values of the depth ratio, n, are shown beside each curve. When both fluids have the same viscosity ($m = 1$) the leading, interfacial mode is neutrally stable. (*a*) Viscosity ratio, $m = 1$; (*b*) Viscosity ratio, $m = 2$.

by Renardy (1987*a*)

$$(\Phi_j, \Phi_k)_h = \frac{(1+n)}{2}(\Phi_j, \Phi_k)_o + \overline{h_j} h_k. \tag{2.12}$$

We call the above inner product the h-norm. The factor $(1+n)/2$ pre-multiplies the term $(\Phi_i, \Phi_j)_o$ so that $\|v\|_h^2$ at R', α', m and n is equal to $\|v\|_h^2$ at R', α', $1/m$ and $1/n$. We have examined the use of other norms, see South (1997) but the h-norm seems best suited to our purposes because the interfacial term of the h-norm emulates the interfacial term, $I(t)$, of the energy rate equation. This is discussed in §3.

The h-norm inner product is mathematically well defined and produces a convergent function $G(t)$, (where $G(t)$ in (2.8) is now defined using the h-norm). This can be seen in figure 4 where we have shown that in order to find $G(t)$ it is sufficient to include modes associated with eigenvalues up to and including the confluence of the two-fluid A, P, S_1 and S_2 branches in the expression for the general disturbance. Like $G(t)$ for single-fluid flows, $G(t)$ for two-fluid flows has a local maximum at time $t = t^{\max}$, which we denote for future reference by $G^{\max}$.

Single-fluid flow results show that $G^{\max}$ is significantly reduced if the initial disturbance does not include the leading shear mode, see Hooper & Grimshaw (1996). Results for two-fluid flows reveal that $G^{\max}$ is significantly reduced by excluding either the interfacial mode or the leading shear mode, see figure 4. Therefore in two-fluid flow systems, it is sometimes the leading shear mode that is more important for growth than the interfacial mode. Of course, because of mode-crossing, it is difficult to define one particular mode as the interfacial mode when m is significantly different from unity.

Figure 5 shows the growth function $G(t)$ based upon the h-norm for four different flows. In figure 5(*a*), the interfacial mode is neutrally stable and the shear modes are stable so that as $t \to \infty$, $G(t) \to C$ where C is the absolute height of the interface $|a_0 h_0|^2$. In figure 5(*b*) the interfacial mode is unstable when $n = 1$ so $G(t) \to \infty$ as $t \to \infty$.

The effect of changing n on $G^{\max}$ is shown in figure 6. The h-norm is a modification of the original energy norm, $\|.\|_o$, a norm which is directly comparable to the single-fluid energy norm. The boundary conditions at each wall means that the interfacial term tends to zero as the interface is brought closer to the wall and we thus expect that h-norm will yield a function $G(t)$ that is equivalent to the single-fluid function $G(t)$ as $n \to \infty$ or $n \to 0$. This is confirmed by the results in figure 6.

The h-norm does not represent an energy norm. Davis & Homsy (1980) call the

https://doi.org/10.1017/S0022112098003577 Published online by Cambridge University Press

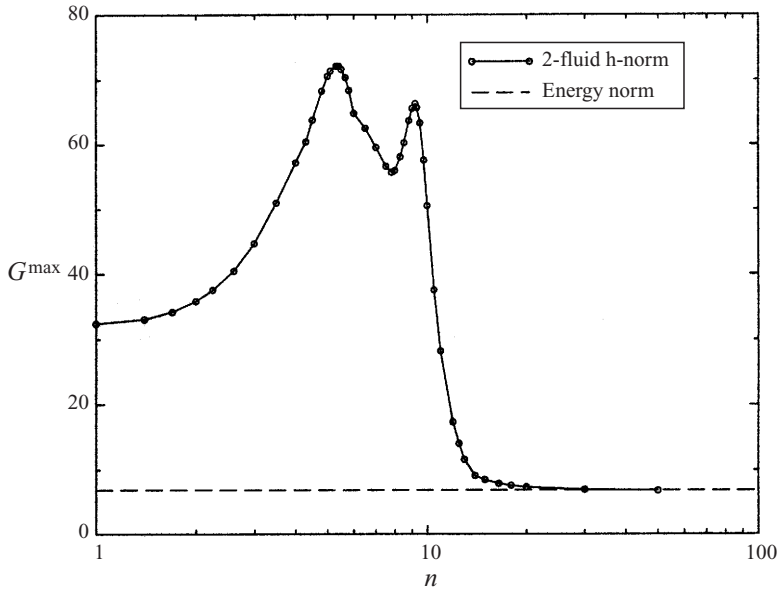


FIGURE 6. G^{max} versus n when $G(t)$ is based upon the h-norm, $m = 1$, $R' = 1000$ and $\alpha' = 1$. The dashed line represents the corresponding single-fluid energy norm G^{max} value.

h-norm the generalized energy of the system. It is difficult, however, to interpret the interfacial component of the h-norm in terms of disturbance energy. In §3 we study the adjoint Orr–Sommerfeld equation and the energy rate for two-fluid flows. We examine similarities between the interfacial terms of the h-norm, the biorthogonality condition for the Orr–Sommerfeld eigenmodes and the adjoint eigenmodes, and the energy rate equation. From the observed similarities we conclude that the h-norm reflects the energy of the whole system of two-fluid flows in that it includes both the kinetic energy of the disturbance velocity field of the two fluids and a term which represents the energy that can be transferred to the disturbance due to the presence of the interface.

3. The adjoint system and energy rate equation for two-fluid flows

In single-fluid flows, the disturbance which maximizes the energy at large time is $\hat{\boldsymbol{\phi}}_1$, the adjoint of the leading eigenvector $\boldsymbol{\phi}_1$ (see Hooper & Grimshaw 1996). The adjoint eigenvector can be found from matrix inversion and is given by

$$\hat{\boldsymbol{\phi}}_1 = U\hat{\boldsymbol{a}}_1 \quad \text{where} \quad \hat{\boldsymbol{a}}_1 = \boldsymbol{H}^{-1}\boldsymbol{e}_1 \tag{3.1}$$

where $\boldsymbol{H}$ is the matrix constructed using the energy inner product for single-fluid flows and $\boldsymbol{e}_1$ is the unit vector $(1, 0, 0, \ldots, 0)^T$.

The adjoint eigenfunction can also be found from the solution of the adjoint Orr–Sommerfeld equation,

$$\psi^{\mathrm{iv}} - \alpha^2\psi'' + \alpha^4\psi = \mathrm{i}\alpha R\{(U - c)(\mathrm{D}^2 - \alpha^2)\psi + 2U'\psi'\}, \tag{3.2}$$

with

$$\psi(\pm 1) = \psi'(\pm 1) = 0.$$

https://doi.org/10.1017/S0022112098003577 Published online by Cambridge University Press

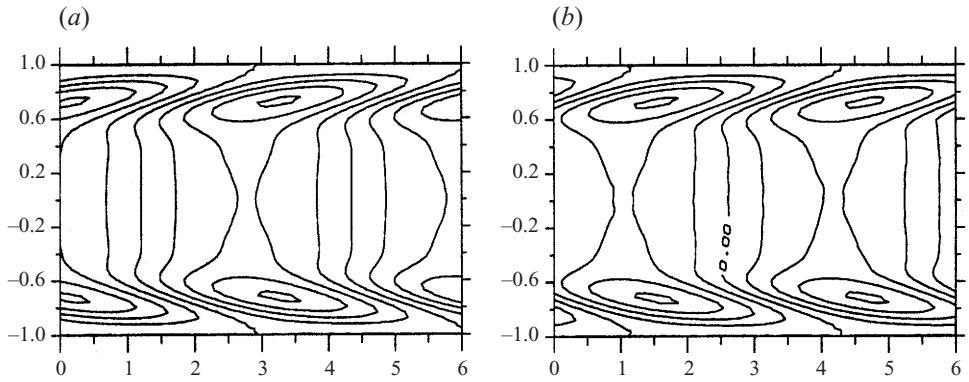


FIGURE 7. Streamfunction contour plots of (*a*) the conjugate of the leading adjoint mode and (*b*) the initial disturbance which leads to $G(t)$ when t is large ($t = 80$) for single-fluid plane Poiseuille flow disturbances when $R = 1000$ and $\alpha = 1$.

The eigenfunctions $\{\phi_j\}$ of the Orr–Sommerfeld equation and the adjoint eigenfunctions $\{\psi_k\}$ satisfy the following biorthogonality condition:

$$\int_{-1}^{1} \phi_j(\mathrm{D}^2 - \alpha^2)\psi_k \mathrm{d}y = \delta_{jk}. \tag{3.3}$$

The integral in equation (3.3) is equivalent to the energy inner product $(\phi_j, \psi_k)_0$. Hence the adjoint eigenvector, $\hat{\boldsymbol{\phi}}_1$ found from matrix inversion (see equation (3.1)) and the leading adjoint eigenvector of (3.2) are the same. This is illustrated in figure 7 where we see that the leading adjoint mode is the same as the disturbance associated with maximum energy growth at large time.

The two-fluid adjoint stability equations when both fluids have the same density and surface tension is zero are

$$\psi^{\mathrm{iv}} - 2\alpha^2\psi'' + \alpha^4\psi = \mathrm{i}\alpha R\{(U_1 - c)(\mathrm{D}^2 - \alpha^2)\psi + 2U_1'\psi'\}, \tag{3.4}$$

$$\omega^{\mathrm{iv}} - 2\alpha^2\omega'' + \alpha^4\omega = \frac{\mathrm{i}r\alpha R}{m}\{(U_2 - c)(\mathrm{D}^2 - \alpha^2)\omega + 2U_2'\omega'\}, \tag{3.5}$$

$$\psi(1) = \psi'(1) = \omega(-n) = \omega'(-n) = 0, \tag{3.6a}$$

$$\psi(0) = \omega(0), \tag{3.6b}$$

$$\psi'(0) = \omega'(0), \tag{3.6c}$$

$$\psi''(0) + \alpha^2\psi(0) = m\{\omega''(0) + \alpha^2\omega(0)\}, \tag{3.6d}$$

$$(\psi'''(0) - 3\alpha^2\psi'(0)) - \frac{U_1'(0)}{(U(0) - c)}(\psi''(0) + \alpha^2\psi(0)) = m\left\{(\omega'''(0) - 3\alpha^2\omega'(0)) - \frac{U_2'(0)}{(U(0) - c)}(\omega''(0) + \alpha^2\omega(0))\right\}, \tag{3.6e}$$

where ψ is the adjoint function in the upper fluid and ω is the adjoint function in the lower fluid.

The original and adjoint eigenfunctions are related through the biorthogonality

https://doi.org/10.1017/S0022112098003577 Published online by Cambridge University Press

condition which for two-fluid flows is

$$\int_0^1 \mathrm{D}\phi_j \mathrm{D}\psi_k + \alpha^2 \phi_j \psi_k \mathrm{d}y + \int_{-n}^0 \mathrm{D}\chi_j \mathrm{D}\omega_k + \alpha^2 \chi_j \omega_k \mathrm{d}y + \frac{1}{\mathrm{i}\alpha R} \frac{(\mathrm{D}\phi_j - \mathrm{D}\chi_j)}{(U_0 - c_k)} (\mathrm{D}^2\psi_k + \alpha^2 \psi_k)|_{y=0} = \delta_{jk}. \quad (3.7)$$

The left-hand side of (3.7) defines an inner product $(\overline{\Phi}, \Psi)_b$, where $\Phi = (\phi, \chi)$ and $\Psi = (\psi, \omega)$. The inner product used in the construction of the h-norm, see equation (2.12), is similar to the inner product $(\Phi_j, \Phi_k)_b$. This becomes clear when we use the boundary conditions of (2.3) and the kinematic condition, (2.3) to show that the interfacial term of $(\Phi_j, \Phi_k)_b$,

$$\frac{1}{\mathrm{i}\alpha R} \frac{(\mathrm{D}\overline{\phi_j} - \mathrm{D}\overline{\chi_j})}{(U_0 - c_k)} (\mathrm{D}^2\phi_k + \alpha^2 \phi_k)|_{y=0}, \quad (3.8)$$

can be written in the form

$$M_k \overline{h_j} h_k, \quad (3.9)$$

where

$$M_k = \frac{1}{\mathrm{i}\alpha R} (U_1' - U_2') \left. \frac{(\mathrm{D}^2\phi_k + \alpha^2 \phi_k)}{\phi_k} \right|_{y=0}. \quad (3.10)$$

The inner product used in the construction of the h-norm is equivalent to the inner product defined by $(\Phi_j, \Phi_k)_b$ with M_k replaced by unity $\forall k$. Because of this similarity between $(\Phi_j, \Phi_k)_b$ and $(\Phi_j, \Phi_k)_h$ used in the construction of the h-norm, we expect at large time the disturbance that gives maximum growth using the h-norm to be very similar to the leading adjoint eigenmode. Figure 8 shows that this is indeed true.

We also note that there is a clear similarity between the interfacial term of $(\Phi_j, \Phi_k)_b$ of (3.8) and the interfacial term, $I(t)$, of the energy rate equation. This is more apparent when $I(t)$ is written in terms of the disturbance streamfunction and given by

$$\mathrm{Re}\left\{ \frac{1}{R} (\mathrm{D}\overline{\psi} - \mathrm{D}\overline{\phi})(\mathrm{D}^2\phi + \alpha^2 \phi)|_{y=0} \right\}. \quad (3.11)$$

Both interfacial terms, $I(t)$ and (3.8), arise when one integrates across the linearized interface at $y = 0$ and are due to the discontinuity in viscosity at that point. The multiplicative term, $1/\mathrm{i}\alpha(U_0 - c_k)$, which appears in (3.8) but not in $I(t)$ is related to the operator $(\mathrm{d}/\mathrm{d}t)^{-1}$ which is the operator required to transform the energy rate equation into an energy equation.

Because the two terms arise in an identical way and are so similar, it seems reasonable to conclude that the interfacial term of the inner product, $(\Phi_j, \Phi_k)_b$ contains the energy transferred to the disturbance via the interface. This term can be either positive or negative. It is replaced in the h-norm by the positive definite term $M|h|^2$ where M is 1. Smaller values of M would place less emphasis on the interfacial energy component as compared to the kinetic energy component of $G(t)$. The close similarity as shown in figure 8, however, between the initial disturbance that leads to $G(t)$ at large time and the leading adjoint eigenmode shows that a choice of $M = 1$ is reasonable for the flow parameters chosen. The values of M_k for the eigenfunctions of the two-fluid Orr–Sommerfeld equation when $\alpha' = 1, R' = 1000, m = 2$ and $n = 1, 2$ are found to be $O(10^{-1})$ for eigenfunctions with eigenvalues along the S_1 and S_2 branches of the eigenvalue distribution, see figure 4, and $O(10^{-2})$ for eigenfunctions

https://doi.org/10.1017/S0022112098003577 Published online by Cambridge University Press

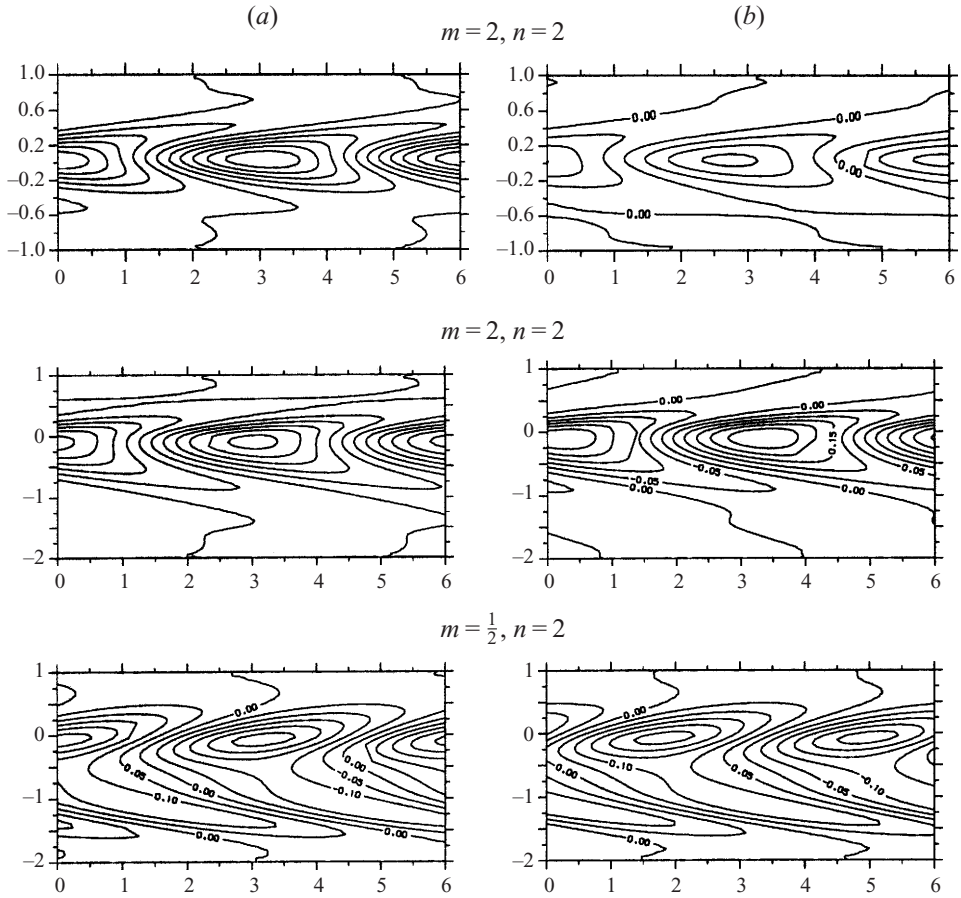


FIGURE 8. Streamfunction contour plots of (*a*) the conjugate of the leading two-fluid adjoint mode and (*b*) the initial disturbance which leads to $G(t)$ (defined using the h-norm) for large time ($t = 80$) for two-fluid plane Poiseuille flow disturbances when $R' = 1000, \alpha' = 1$ and different values of m and n.

with eigenvalues scattered above the S_1 and S_2 branches. This suggests that values of M of less than 1 would also lead to convergent results and that these results would be quantitatively closer to the maximum kinetic energy growth of the disturbance. This is explored in §4.

An inspection of the energy rate equation shows that one would expect the Reynolds stress mechanism and not the interfacial term, $I(t)$, to lead to a growth in $G(t)$. This is because most of the energy growth due to $I(t)$ in the energy rate equation has been incorporated into $G(t)$ by use of the h-norm. In §4 we consider two initial disturbances that give maximum energy growth. We calculate $I(t)$ for these disturbances and show that $I(t)$ is negligible for all time. This supports the expectation that the mechanism for energy growth in $G(t)$ is the Reynolds stress only.

4. Results

The function $G(t)$ defined using the h-norm consists of two components: the kinetic energy growth within both fluids and the interfacial growth. We wish to examine the

https://doi.org/10.1017/S0022112098003577 Published online by Cambridge University Press

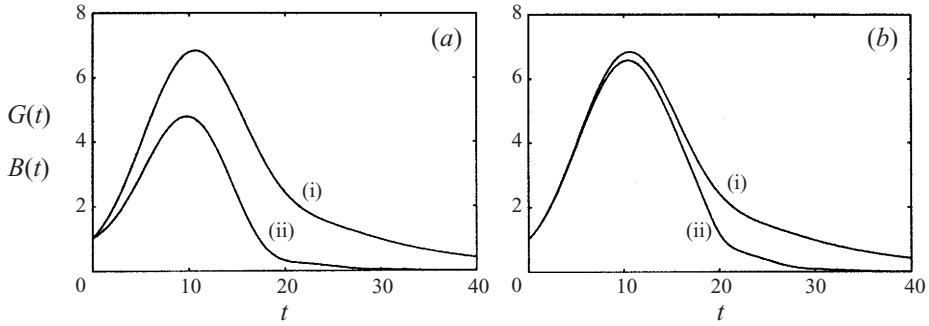


FIGURE 9. Comparing single-fluid $G(t)$ (line (i)) and two-fluid $B(t)$ (line (ii)), (a) as calculated with the h-norm and (b) as calculated with the modified h-norm for $M = 0.1$. For all curves, $R = 1000$, $\alpha = 1$ and in the two-fluid configurations, $m = 1$ and $n = 1$.

growth of the kinetic energy component separately. Thus we note that the h-norm can be written in the following way:

$$\|v(y,t)\|_h^2 = \frac{(1+n)}{2}\left\{\int_0^1 \left|\frac{\partial v_1}{\partial y}\right|^2 + \alpha^2|v_1|^2 \mathrm{d}y + \int_{-n}^0 \left|\frac{\partial v_2}{\partial y}\right|^2 + \alpha^2|v_2|^2 \mathrm{d}y\right\} + |v_3|^2, \quad (4.1)$$

where

$$v_1 = \sum_{p=1}^{K} a_p \phi_p(y) \mathrm{e}^{-\mathrm{i}\alpha c_p t}, \quad v_2 = \sum_{p=1}^{K} a_p \chi_p(y) \mathrm{e}^{-\mathrm{i}\alpha c_p t}, \quad v_3 = \sum_{p=1}^{k} a_p h_p \mathrm{e}^{-\mathrm{i}\alpha c_p t}$$

and $(\phi_p(y), \chi_p(y), h_p)^T$ is the compound eigenvector of the two-fluid Orr–Sommerfeld equations defined in §2.1. Once $G(t)$ and hence $\{a_p\}$ are known we can isolate each term v_1, v_2, v_3 that make up $G(t)$.

We define a scaled kinetic energy growth function $B(t)$ which is normalized with respect to the initial kinetic energy so that

$$B(t) = \frac{G(t) - |v_3(t)|^2}{G(0) - |v_3(0)|^2}. \quad (4.2)$$

The function $B(t)$ allows us to compare energy growth of the two-fluid system with energy growth in the single-fluid system. Of course the energy growth found may not be the maximum kinetic energy growth possible in the two-fluid system because the function maximized involves kinetic energy plus an interfacial $|h|^2$ term, but the comparison does give some indication of possible kinetic energy growth in two-fluid systems. Despite this caveat, $B(t)$ in the single-fluid limit compares well with the single-fluid energy growth function $G(t)$ as can be seen in figure 9(a). The two graphs do not quantitatively match because the h-norm is not simply a kinetic energy norm but they do match qualitatively. This qualitative match is maintained wherever the interface is positioned (in figure 9 it is in the centre of the channel) although $B^{\max}$ does show approximately 10% variation with n. Closer agreement is found when the inner product of the h-norm is modified to

$$(\Phi_j, \Phi_k)_h = \frac{(1+n)}{2}(\Phi_j, \Phi_k)_o + M\overline{h_j}h_k \quad (4.3)$$

with M less than 1. Care must be taken so that the norm $\|v(t)\|$ defined with the above inner product converges once the series expansion for $v(t)$ includes a finite number

https://doi.org/10.1017/S0022112098003577 Published online by Cambridge University Press

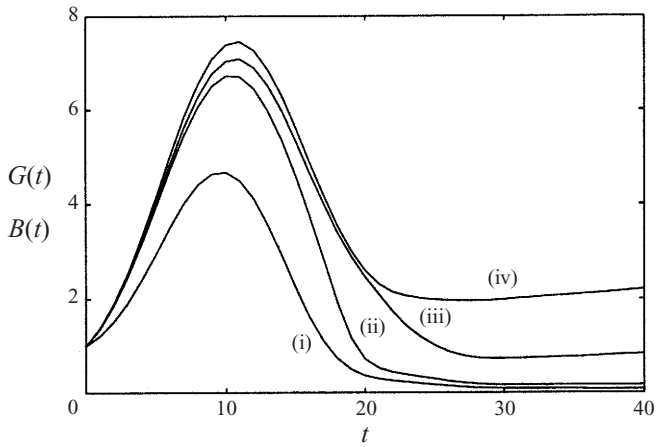


FIGURE 10. Energy growth function $B(t)$ defined using the modified h-norm of (4.3) when $R' = 1000$, $\alpha' = 1$, $m = 2$, $n = 1$ and (i) $M = 1$, (ii) $M = 0.1$, (iii) $M = 0.02$. The modifed h-norm growth function $G(t)$ with $M = 0.02$ is shown in curve (iv). Note that the interfacial mode is unstable for these flow parameters and so all curves (i)–(iv) will grow as $t \to \infty$.

of terms. We already know that $M = 0$ leads to problems of non-convergence. Study of the inner product associated with the biorthogonality condition, $(\overline{\Phi_j}, \Phi_k)_b$, suggests that values of M between 0.01 and 0.1 should produce a convergent norm when $\alpha' = 1, R' = 1000$, $m = 2$ and $n = 1, 2$. We find that this is indeed the case. As expected, as M becomes smaller, more emphasis is placed on the kinetic energy growth of the disturbance and when $m = 1$, $B(t)$ approaches the single-fluid energy growth function $G(t)$, as can be seen in figure 9(b) with $M = 0.1$. As pointed out by a referee, (3.10) suggests that we choose a value of M which is proportional to $(m - 1)$, so that when $m = 1$ the weighting given to the interface vanishes. We have not explored this option but it seems a sensible way to proceed. We have shown, however, that even with a non-zero value of M, one can almost recover the true values of energy growth, as shown in figure 9, as long as M is sufficiently small.

We also look at the two-fluid configuration when $m = 2$ and $n = 1$ at $R' = 1000$ and $\alpha' = 1$. Figure 10 shows the corresponding kinetic energy growth function $B(t)$ found using the modified h-norm when M is 1, 0.1 and 0.02. Again, as M becomes smaller, more emphasis is placed on the kinetic energy growth component of $G(t)$ and less emphasis on the interfacial term of $G(t)$. Furthermore, the two curves, $G(t)$ and $B(t)$, calculated using the h-norm when M is 0.02 are almost identical in the transient growth phase, see lines (iii) and (iv) of figure 10. In figure 11 we show growth curves for the two-fluid flow when $R' = 1000$, $\alpha' = 1$, $m = 10$ and $n = 5$ (compare figure 13). Figure 11 shows three lines: lines (i) and (ii) are respectively $G(t)$ and $B(t)$ calculated using the modified h-norm when $M = 0.02$ and line (iii) is $G(t)$ calculated using the original energy norm of equation (2.6) when the interfacial mode is excluded. We see that all three curves are extremely close. We have found similar results in the transient growth phase of other flows such as the flow configuration of figure 10 (when $m = 2$, $n = 1$, $R' = 1000$ and $\alpha' = 1$). For the two-fluid flows studied here, the transient energy growth is a shear mode phenomenon and the presence of the interfacial mode is of secondary importance.

The maximum energy growth of a disturbance must lie between the curves $G(t)$ and $B(t)$ calculated using the modified h-norm. As $M \to 0$, the curves $G(t)$ and $B(t)$

https://doi.org/10.1017/S0022112098003577 Published online by Cambridge University Press

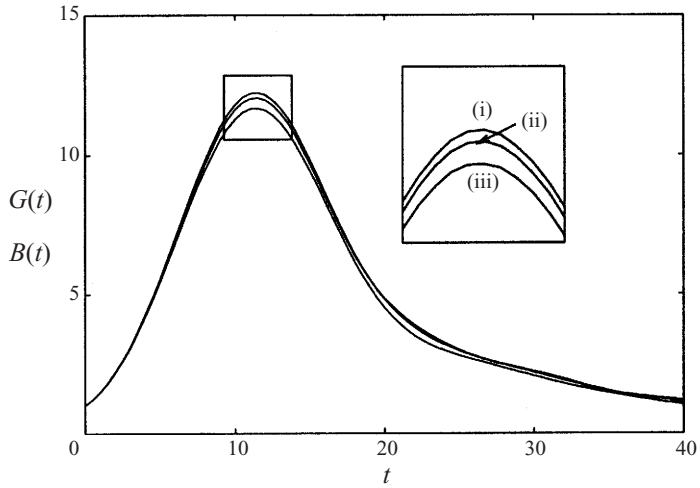


FIGURE 11. Disturbance growth for two-fluid flow when $R' = 1000$, $\alpha' = 1$, $m = 10$ and $n = 5$. Lines (i) and (ii) are the curves $G(t)$ and $B(t)$, respectively, calculated using the modified h-norm when $M = 0.02$. Line (iii) is $G(t)$ calculated using the original energy norm when the interfacial mode is excluded from the disturbance.

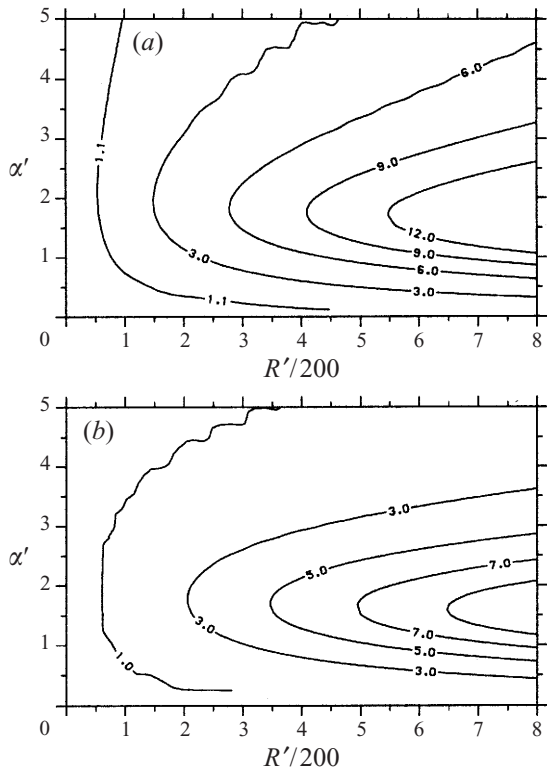


FIGURE 12. (*a*) $G^{\max}(R', \alpha')$ contours for single-fluid plane Poiseuille flow and (*b*) two-fluid $B^{\max}(R', \alpha')$ contours for the single fluid limit ($m = 1$) when $n = 1$. (The wiggles apparent on some of the contour lines are believed to be a numerical artefact.)

https://doi.org/10.1017/S0022112098003577 Published online by Cambridge University Press

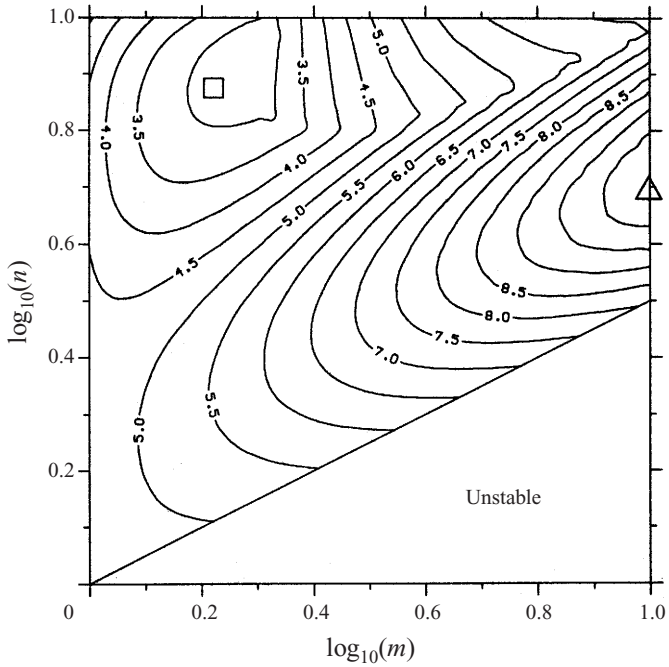


FIGURE 13. $B^{\max}(m,n)$ contours, $R' = 1000$ and $\alpha' = 1$: □, minimum found at $m \approx 1.6, n \approx 7.4$; △, maximum found at $m = 10$ and $n = 5$.

tend to coalesce. If M becomes too small, however, problems with non-convergence re-emerge. The smallest value of M will depend on the flow parameters of the system. We conclude that the modified h-norm with M chosen to be the smallest value of M to ensure convergent results is representative of the energy norm for two-fluid flows if the calculated curves for $G(t)$ and $B(t)$ are sufficiently close (as is the case with lines (iii) and (iv) of figure 10 for $t < 20$ when $M = 0.02$ and lines (i) and (ii) of figure 11, $\forall t$). We note, however, that the qualitative behaviour of the results in the transient growth phase is the same whether the modified or unmodified h-norm is used. All further results in this section are presented for the unmodified h-norm with $M = 1$.

The similarity of $B(t)$ and single-fluid $G(t)$ is further emphasized in figure 12 which shows $G^{\max}(R', \alpha')$ for single-fluid plane Poiseuille flow and $B^{\max}(R', \alpha')$ in the single-fluid limit of the two-fluid configuration. As with single-fluid $G(t)$ there are regions of no energy growth (at low Reynolds number) and the wavenumber at which most growth is found is approximately 2.

In figure 13, $B^{\max}$ contours in the (m,n)-plane are shown for fixed values of R' and α'. There is a maximum of the $B^{\max}$ contours at $m > 10$ and $n \approx 5$ and a minimum at $n = 7.4$ and $m = 1.6$. The streamfunctions of the disturbances associated with the maximum and minimum $B^{\max}$ disturbances are given in figure 14. Both disturbances show circulation around the interface but the disturbance associated with the largest growth (figure 14*a*) also has separate circulation 'cells' at the channel walls. These wall circulation 'cells' oppose the velocity gradient of the basic flow. Similar wall circulation structures are found in single-fluid flow (see figure 7) where they are most pronounced for the disturbance that creates most transient growth (with fixed R') at $\alpha' \approx 2$. The disturbance that produces least energy growth (as shown in figure 14*b*) shows much weaker wall circulation structures. It is likely that the

https://doi.org/10.1017/S0022112098003577 Published online by Cambridge University Press

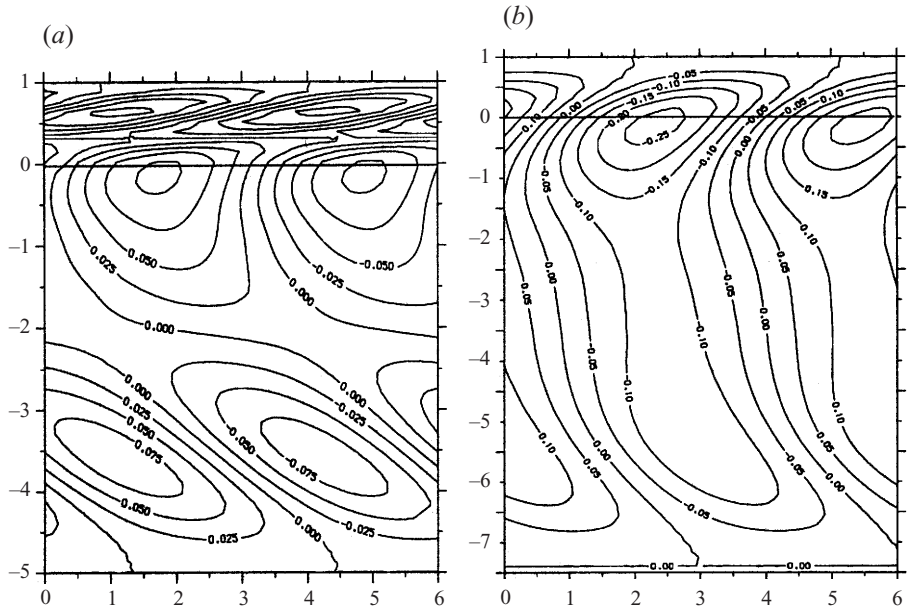


FIGURE 14. Streamfunction contour plots at $R' = 1000$, $\alpha' = 1$ for the disturbances that lead to (*a*) $B^{\max}$ when $m = 10$ and $n = 5$ and (*b*) $B^{\max}$ when $m = 1.6$ and $n = 7.4$.

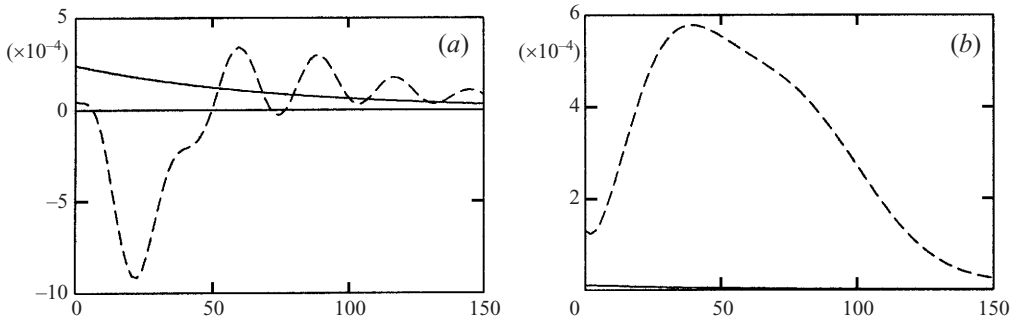


FIGURE 15. The interfacial term of the energy equation $I(t)$ when $R' = 1000$, $\alpha' = 1$: (*a*) $m = 10$, $n = 5$ and (*b*) $m = 1.6$, $m = 7.4$. The dashed line refers to $I(t)$ when the initial disturbance comprises a series expansion of eigenmodes which lead to $B^{\max}$ (see figure 14) and the solid line refers to $I(t)$ when the initial disturbance comprises the interfacial mode only.

two-fluid disturbance which grows the most uses this streamline tilting mechanism which is also apparent in single-fluid flows.

We calculate $I(t)$ for the two configurations highlighted in figure 13. Figure 15 shows $I(t)$ for two disturbances: I_0 made up of the interfacial mode only and I_K, the modal sum whose energy grows to $B^{\max}$. When the disturbance is defined as a series expansion of modes (as in $I_K(t)$) we see in figure 15(*a*) that the interfacial term can act to increase or decrease the rate of change of kinetic energy as a function of time. In figure 15(*a*) $I_0(t)$ and $I_K(t)$ are $O(10^{-4})$ whereas the disturbance that leads to $B^{\max}$ requires an energy growth rate of $O(10^{-1})$. The same difference in magnitudes is found at the configuration for which figure 15(*b*) is drawn.

We conclude from the above results that the Reynolds stress term of the energy rate equation is the most important energy growth mechanism for non-modal disturbances

https://doi.org/10.1017/S0022112098003577 Published online by Cambridge University Press

in two-fluid flows. The energy transfer caused by the Reynolds stress is enhanced by the streamline tilting apparent in the streamline plots of the disturbance. This is the same mechanism found for energy transfer in transient growth of single-fluid flows. We also conclude, for the two-fluid flows studied in this paper, that the transient energy growth is a shear mode phenomenon and that the presence of the interfacial mode is of secondary importance.

We would like to thank Dr Yuriko Renardy for her suggestion to use the h-norm to resolve the problem of non-convergence of the energy norm in two-fluid flows. Matthew South acknowledges the support of a UWE bursary throughout the course of this work.

REFERENCES

Butler, K. M. & Farrell, B. F. 1992 Three-dimensional optimal perturbations in viscous shear flow. *Phys. Fluids* A **4**, 1637–1650.

Davis, S. H. & Homsy, G. M. 1980 Energy stability theory for free-surface problems: buoyancy-thermocapillary layers. *J. Fluid Mech.* **98**, 527–553.

Farrell, B. F. 1988 Optimal excitation of perturbations in viscous shear flow. *Phys. Fluids* **31**, 2093.

Hooper, A. P. & Grimshaw, R. 1996 Two-dimensional disturbance growth of linearly stable viscous shear flows. *Phys. Fluids* **8**, 1424–1432.

Joseph, D. D. 1988 Two fluids heated from below. *Energy Stability and Convection*. Pitman Research Notes, no. 168, pp. 364–382.

Mack, L. M. 1976 A numerical study of the temporal eigenvalue spectrum of Blasius boundary layer flow. *J. Fluid Mech.* **73**, 221.

Reddy, S. C. & Henningson, D. S. 1993 Energy growth in viscous channel flow. *J. Fluid Mech.* **252**, 209–238.

Renardy, Y. 1987*a* The thin-layer effect and interfacial stability in a two layer Couette flow with similar fluids. *Phys. Fluids* A **30**, 1627–1637.

Renardy, Y. 1987*b* Viscosity and density stratification in vertical Poiseuille flow. *Phys. Fluids* A **30**, 1638–1648.

South, M. J. 1997 Linear energy growth in two-fluid Poiseuille flow. PhD thesis, University of the West of England.

Trefethen, L. N., Trefethen, A. E., Reddy, S. C. & Driscoll, T. A. 1993 Hydrodynamic stability without eigenvalues. *Science* **261**, 578–584.

Yih, C. S. 1967 Instability due to viscosity stratification. *J. Fluid Mech.* **27**, 337–352.

https://doi.org/10.1017/S0022112098003577 Published online by Cambridge University Press